THE ASTROPHYSICAL JOURNAL, 462:L17–L21, 1996 May 1

SPECTROSCOPIC CONFIRMATION OF A POPULATION OF NORMAL STAR-FORMING GALAXIES AT REDSHIFTS $z > 3$[1]

CHARLES C. STEIDEL,[2,3,4] MAURO GIAVALISCO,[5,6] MAX PETTINI,[7] MARK DICKINSON,[8] AND KURT L. ADELBERGER[2]
Received 1995 December 17; accepted 1996 February 20

ABSTRACT

We report the discovery of a substantial population of star-forming galaxies at $3.0 \lesssim z \lesssim 3.5$. These galaxies have been selected using color criteria sensitive to the presence of a Lyman continuum break superposed on an otherwise very blue far-UV continuum, and then confirmed with deep spectroscopy on the W. M. Keck telescope. The surface density of galaxies brighter than $\mathcal{R} = 25$ with $3.0 \lesssim z \lesssim 3.5$ is 0.4 ± 0.07 galaxies arcmin^{-2}, approximately 1.3% of the deep counts at these magnitudes; this value applies both to "random" fields and to fields centered on known QSOs. The corresponding comoving space density is approximately half that of luminous ($L \gtrsim L^*$) present-day galaxies. Our sample of $z > 3$ galaxies is large enough that we can begin to detail the spectroscopic characteristics of the population as a whole. The spectra of the $z > 3$ galaxies are remarkably similar to those of nearby star-forming galaxies, the dominant features being strong low-ionization interstellar absorption lines and high-ionization stellar lines, often with P Cygni profiles characteristic of Wolf-Rayet and O star winds. Lyα emission is generally weak (less than 20 Å rest equivalent width) and is absent for more than 50% of the galaxies. We assign approximate mass scales to the galaxies using the strengths of the heavily saturated interstellar features and find that, if the line widths are dominated by gravitational motions within the galaxies, the implied velocity dispersions are 180 km s$^{-1} \leq \sigma \leq$ 320 km s^{-1}, in the range expected for massive galaxies. The star formation rates, which can be measured directly from the far-UV continua, lie in the range 4–25 $h_{50}^{-2}\ M_\odot$ yr^{-1} (for $q_0 = 0.5$), with 8.5 $h_{50}^{-2}\ M_\odot$ yr^{-1} being typical. Together with the morphological properties of the $z > 3$ galaxy population, which we discuss in a companion paper, all of these findings strongly suggest that we have identified the high-redshift counterparts of the spheroid component of present-day luminous galaxies. In any case, it is clear that massive galaxy formation was already well underway by $z \sim 3.5$.

Subject headings: cosmology: observations — galaxies: distances and redshifts — galaxies: evolution — galaxies: formation

1. INTRODUCTION

Several years ago we embarked on a program to assess the presence of "normal" star-forming galaxies at redshifts $z > 3$ using a custom suite of broadband filters (dubbed U_n, G, and $\mathcal{R}$; see Steidel & Hamilton 1993) designed to reach very faint apparent magnitudes with accurate colors. The technique rests on only two assumptions about the spectra of high-redshift galaxies: (1) a roughly flat spectrum ($f_\nu \propto \nu^0$) in the far-UV where the flux is dominated by emission from massive stars and (2) a pronounced spectral break at 912 Å (the Lyman limit in the galaxy rest frame) due to the combination of the intrinsic stellar energy distributions, the inherent opacity of the galaxies to Lyman continuum photons, and the effects of intervening absorbers (see Steidel & Hamilton 1992, 1993; Steidel, Pettini, & Hamilton 1995 [Papers I, II, III] for an extensive discussion of the technique; see also Madau 1995). The filters are tuned to selecting objects with redshifts in the range $3.0 \lesssim z \lesssim 3.5$, where the U_n passband falls mostly shortward of the Lyman limit and the G band is not severely blanketed by the Lyα forest (at higher redshifts this blanketing can make it very difficult to distinguish a spectral break from an intrinsically red spectral energy distribution).

While earlier work (Guhathakurta, Tyson, & Majewski 1990) had shown that Lyman break galaxies do not dominate the galaxy counts at faint apparent magnitudes, these constraints were too weak to rule out the presence of a substantial population of such objects among the more prominent foreground blue galaxies. Our first searches were directed at the fields of QSOs with known Lyman limit absorption systems at $z > 3$; these could then be used as templates to guide one (eventually) to galaxies in the general field, or at least to test the feasibility of detecting normal galaxies at such extreme redshifts. In Paper III we discussed together the properties of both QSO absorbers and candidates in the general field, since QSO absorbers are apparently drawn from the population of relatively luminous (but otherwise normal) field galaxies, at least at smaller redshifts (see Steidel, Dickinson, & Persson 1994). We found the surface density to be the same within the errors in all five fields studied, and we reported a surface density of robust candidates for Lyman break galaxies of $\approx$0.5 arcmin^{-2} to an apparent magnitude limit of $\mathcal{R} = 25$.

Since the completion of Paper III, we have been working on extending the $U_nG\mathcal{R}$ imaging technique to more random (i.e., non-QSO) fields and, most important, on following up the candidates with deep spectroscopy on the Keck telescope. In

[1] Based in large part on observations obtained at the W. M. Keck Observatory, which is operated jointly by the California Institute of Technology and the University of California.

[2] Palomar Observatory, California Institute of Technology, Mail Stop 105-24, Pasadena, CA 91125.

[3] Alfred P. Sloan Foundation Fellow.

[4] NSF Young Investigator.

[5] Observatories of the Carnegie Institution of Washington, 813 Santa Barbara Street, Pasadena, CA 91101.

[6] Hubble Fellow.

[7] Royal Greenwich Observatory, Madingley Road, Cambridge CB3 OEZ, UK.

[8] Space Telescope Science Institute, 3700 San Martin Drive, Baltimore, MD 21218.

TABLE 1

SUMMARY OF CANDIDATES OBSERVED SPECTROSCOPICALLY

Object	$\mathcal{R}$	$G-\mathcal{R}$	U_n-G	$\mathcal{R}-K$	Redshift[a]	W_λ(Lyα)[b]
0347−383 N5	23.82	0.65	>2.85	2.5	3.243	6
0000−263 C02[M]	24.06	1.23	>2.45	...	star	...
0000−263 C04	23.71	1.00	>2.96	...	3.789	(QSO)
0000−263 C06	25.49	0.96	>1.75	...	3.202	3
0000−263 C09	24.44	0.00	>3.36	3.9	3.428[c]	355
0000−263 C11	25.30	0.50	>2.32	3.2	3.135	8
0000−263 C13	25.38	0.90	>1.75	...	3.238	<0
0000−263 C14	24.54	0.77	>2.45	...	3.022	7
0000−263 C16	24.47	0.85	>2.54	...	3.056	18
0000−263 C17	25.35	0.68	>1.97	...	3.169	<0
0000−263 C19	25.26	0.99	>2.17	...	...	...
0000−263 C21[M]	23.79	1.24	1.85	...	star	...
0000−263 C23	23.93	0.51	1.73	...	3.199	<0
0000−263 C25	25.08	0.60	>1.78	...	3.342	<0
0000−263 C26	25.77	0.26	>2.13	...	...	...
0000−263 C27[M]	25.00	0.52	1.52	...	2.780	<0
0000−263 C28	24.90	0.70	>1.90	...	...	...
SSA 22 C01	25.50	0.25	>1.93	...	...	...
SSA 22 C03	25.37	0.12	>1.95	...	...	...
SSA 22 C10	24.86	0.21	>2.26	...	3.375	<0
SSA 22 C11	24.82	0.41	>2.18	...	...	...
SSA 22 C12	24.78	0.43	>2.13	...	3.201	3
SSA 22 C14	24.64	0.26	>2.31	...	3.401	<0
SSA 22 C16	24.62	0.46	>2.10	...	...	...
SSA 22 C19	24.58	0.39	>2.50	...	3.019	22
SSA 22 C20	24.52	0.27	>2.55	...	3.019	<0
SSA 22 C24	23.45	0.38	>3.01	...	...	...
SSA 22 D10	21.75	0.52	2.56	...	3.083	(QSO)
SSA 22 D11[M]	21.53	1.13	3.26	...	star	...
SSA 22 D12	20.98	0.87	3.82	...	3.352	(QSO)
2233+131 N1	25.02	0.15	>2.38	[3.0]	3.151[d]	...

NOTE.—Superscript M denotes a marginal candidate on the basis of U_n-G and $G-\mathcal{R}$ colors.

[a] Spectroscopic redshift, when secure.

[b] Rest equivalent width of Lyα emission line for galaxies, in angstroms; values less than zero indicate net absorption at the position of Lyα.

[c] Object "G2" (Giavalisco et al. 1994)—Keck spectrum shows presence of C IV, He II, O VI, and N V emission, hence G2 is probably an AGN.

[d] Spectroscopic confirmation from Djorgovski et al. 1996.

this Letter we report the successful results of our first attempts at spectroscopy of the Lyman break candidates, new $U_nG\mathcal{R}$ imaging in (much larger) random fields which confirms the surface density estimates given in Paper III, and the first measurements of K-band magnitudes for the $z>3$ population.

2. SPECTROSCOPY

The spectra were obtained during the nights of 1995 October 1–2 (UT) and 1995 October 29–30 (UT) with the W. M. Keck telescope and the Low Resolution Imaging Spectrograph (LRIS; Oke et al. 1995). By using multiobject slit masks, each $\sim 4' \times 7'$ (and in one case long-slit spectroscopy), we recorded the spectra of 25 robust candidates for $z>3$ galaxies in three fields: two are QSO fields, 0000−263 and 0347−383, and the third is the Hawaii deep survey field SSA 22 (Lilly, Cowie, & Gardner 1991; Cowie et al. 1994). These observations were made in far from optimum conditions, being either at large air mass (typically 1.8–2.0 for the southern fields) or in gray time (SSA 22); consequently, the spectra we obtained do not reflect the full capabilities of the LRIS+Keck combination.

Candidates in the 0000−263 and 0347−383 fields were selected on the basis of the photometry in Papers I and III, augmented by deeper images of the former field acquired more recently. For the SSA 22 field we used photometry obtained with the Palomar 5 m telescope in 1995 August and described in § 4 below. As the number of available slitlets exceeded the number of robust candidates which could be observed with each mask, we also observed four "marginal" candidates, that is, objects whose colors placed them at or near the boundaries of the color criteria (in either $G-\mathcal{R}$ or U_n-G) outlined in Paper III, for the purpose of possibly improving our selection criteria in future. We summarize the results of the spectroscopy in Table 1, which includes relevant data for all of the candidates, both robust and marginal, which have been attempted to date.

Of the 23 objects identified, 16 are galaxies with $3.01 \le z \le 3.43$ and three are faint QSOs. The other four identified objects were considered to be marginal candidates, in three cases because of red $G-\mathcal{R}$ colors and significant U_n band detections (all three turn out to be halo subdwarf stars). The fourth case, which showed evidence for a spectral break but which had a U_n-G color slightly bluer than our robust candidates, is a galaxy at $z=2.780$. Of the eight robust candidates with undetermined redshifts, none is actually inconsistent with being at $z>3$; in no case do we find a secure spectral feature at a lower redshift (the spectral range covered includes [O II] $\lambda3727$ up to $z<1.4$). Many of these objects exhibit continuum discontinuities ($\sim$0.3–0.6 mag) which are indicative of the onset of the Lyα forest.

To summarize, roughly 70% of the objects which we considered to be robust candidates have been confirmed to have

$3.0 \leq z \leq 3.5$, and the other ~30% are consistent with the same range of redshifts.[9]

3. SPECTRA OF $z > 3$ GALAXIES

In Figure 1 (Plate 3) we have reproduced some examples of Keck spectra of $z > 3$ galaxies, chosen to illustrate the variety of features encountered. In each case we have included for comparison a recent *HST* spectrum of the central starburst region in the Wolf-Rayet galaxy NGC 4214 (Leitherer et al. 1996).

Qualitatively, the similarity between the high-redshift galaxies and local examples of starbursts is striking. In each case the dominant characteristics of the far-UV spectrum are: (1) a flat continuum, (2) weak or absent Lyα emission, (3) prominent high-ionization stellar lines of He II, C IV, Si IV, and N V, and (4) strong interstellar absorption lines due to low-ionization stages of C, O, Si, and Al. These stellar and interstellar lines are the most distinctive spectral features in many of the $z > 3$ galaxies; this makes confirmation of objects at $z > 2$ with optical spectroscopy much more promising than might have been anticipated, even in the absence of strong ultraviolet emission lines. The continuum specific luminosity at 1500 Å of a typical $z > 3$ galaxy in our sample is $L_{1500} = 10^{41}\ h_{50}^{-2}$ ergs s^{-1} Å^{-1} (for $q_0 = 0.5$; three times greater for $q_0 = 0.05$); this is ≈500–1500 times higher (depending on the value of q_0) than the knot of star formation in NGC 4214 observed by Leitherer et al. (1996) and ≈30–100 times higher than the brightest such knots seen in nearby starburst galaxies. Thus, for a "normal" initial mass function (IMF), the far-UV continuum we see in the $z > 3$ objects is produced by the equivalent of $\approx 2\text{–}6 \times 10^5$ O7 stars.

A detailed discussion of the spectra is beyond the scope of this paper; here we limit ourselves to a few preliminary considerations. All of the galaxies in the sample are consistent with unreddened models of young star-forming galaxies (Bruzual & Charlot 1993). The expected dust-free $G - \mathcal{R}$ colors are in the range 0.3–0.9 after accounting for the blanketing of the G band by the Lyα forest (see Madau 1995; Paper III), the same as the observed range in our sample. With the caveat that there are uncertainties in the models of young galaxies (see, e.g., Charlot 1996), we estimate that the maximum reddening allowed in the $G - \mathcal{R}$ color is ~0.4 mag. Taking this as an upper limit, and using the extragalactic reddening curve of Calzetti, Kinney, & Storchi-Bergmann (1994), the extinction at observed $\mathcal{R}$ (rest ~ 1600 Å) would be less than 1.7 mag, or a factor of less than 5. The corresponding optical reddening in the rest frame of the galaxies would be $E(B - V) < 0.3$ mag.

Despite the apparent lack of a large amount of dust, Lyα emission is always much weaker (usually by factors of more than 10) than the ionization-bound, dust-free expectations, given the production of ionizing photons by massive stars which we measure directly from the UV continuum. Reasons for the preferential extinction of Lyα emission have been discussed by, e.g., Charlot & Fall (1993) and Chen & Neufeld (1994); our observations are entirely consistent with the same low (but nonzero) dust content inferred to be present in the high-redshift damped Lyα absorption systems (e.g., Pei, Fall, & Bechtold 1991; Pettini et al. 1994). In the spectra which do show Lyα emission the typical rest-frame equivalent width is $W_{\mathrm{Ly}\alpha} = 3\text{–}20$ Å, but apparently most $z > 3$ galaxies have Lyα emission lines weaker than these values, in striking similarity to nearby star-forming galaxies (e.g., Giavalisco, Koratkar, & Calzetti 1996a). For example, C23 0000−263 in Figure 1 has among the largest implied star formation rates in our sample (as discussed in § 6 below), and yet has no measurable Lyα emission.

The Lyα emission lines and number density that we measure for our galaxies are consistent with the essentially null results of all previous searches for high-z galaxies based on this spectral feature (e.g., Thompson, Djorgovski, & Trauger 1995; Lowenthal et al. 1995; Pettini et al. 1995). Given the star formation rates we derive, the space density of the Lyman break galaxies (§ 6) is also consistent with null results from near-IR surveys (e.g., Pahre & Djorgovski 1995; Mannucci, Beckwith, & McCaughrean 1994) for redshifted Hα, [O III], and [O II] lines. While the near-IR surveys can reach star formation rates comparable to those we observe, the volumes surveyed to date are too small for a significant chance of detection.

While there is a great deal of variety in the strengths of the lines which are predominantly of stellar origin (C IV λ1549, Si IV λλ1393, 1402, and He II λ1640), we find these features to be generally weaker than in the spectra of present-day starbursts. This is probably an abundance effect; these lines are formed predominantly in the winds of massive stars, where both mass-loss rates and wind terminal velocities are known to depend sensitively on metallicity (e.g., Walborn et al. 1995).

The strongest interstellar lines indicated in Figure 1 have typical rest-frame equivalent widths $W_0 \simeq 2\text{–}3.5$ Å. While the interstellar medium of these galaxies has obviously undergone some chemical enrichment, it is not possible to deduce metallicities from our spectra, since the absorption lines in question are undoubtedly heavily saturated. Under these circumstances, values of metallicity anywhere between 0.001 solar and solar are compatible with the line strengths, and higher resolution observations of intrinsically weaker lines are required to measure element abundances (Pettini & Lipman 1995). The equivalent widths of saturated absorption lines are much more sensitive to the velocity dispersion of the gas than to its column density. The observed $W_0 \simeq 2\text{–}3.5$ Å correspond to FWHM ≥ 400–700 km s^{-1}, which in turn imply approximate velocity dispersions $\sigma = 180\text{–}320$ km s^{-1} (slightly higher values apply if rotation is the dominant effect). In any case, if these velocity spreads reflect primarily gravitationally induced motions in the large-scale interstellar medium of the galaxies, the masses implied are comparable to those of present-day luminous galaxies. Smaller masses would result if interstellar shocks, local to the star-forming regions, contribute to the line widths. Spectra of higher signal-to-noise ratio and resolution are required to resolve this question.

4. SURFACE DENSITY OF LYMAN BREAK OBJECTS

In parallel with this spectroscopic follow-up, we have been obtaining deep $U_nG\mathcal{R}$ images of additional fields using the COSMIC camera at the prime focus of the Palomar 5 m telescope with two principal aims: (1) improve the statistics on the surface density of Lyman break objects, by taking advantage of the much larger field of view available to COSMIC (9'.7 × 9'.7, compared to approximately 1'.5 × 1'.5 of most of

[9] We note that an additional Lyman break candidate from our survey has recently been confirmed spectroscopically. In Paper III we proposed that an $\mathcal{R} = 25.0$ galaxy 2''.9 from the line of sight to Q2233+1310 is the $z = 3.15$ damped Lyα absorber, as this is the best candidate Lyman break object in the small field we observed around the QSO. Djorgovski et al. (1996) have serendipitously obtained a spectrum of this candidate showing Lyα emission at the predicted wavelength.

the observations reported in Paper III); and (2) extend this work to random fields, that is, fields which do not include known QSOs, so as to assess whether the surface density deduced in Paper III is typical of the general field.

To this end we have chosen one of the Hawaii deep survey fields, SSA 22, which has also been observed extensively with post-refurbishment *HST* (e.g., Cowie, Hu, & Songaila 1995a) in several pointings, all falling within our Palomar 5 m images. These new $U_n G \mathcal{R}$ images reach depths comparable to those of the data in Paper III, and allow us to be complete in our identification of $z > 3$ galaxies down to $\mathcal{R} = 25.0$. We find a total of 31 robust candidates satisfying the selection criteria outlined in Paper III out of a total of 2340 objects detected to the same apparent magnitude level (the field size in the stacked images was $8'.8 \times 9'.0$). We therefore deduce a surface density of Lyman break candidates of 0.40 ± 0.07 arcmin^{-2} (or 1.44×10^3 degree^{-2}), consistent with (and significantly more accurate than) the value $\approx$0.5 arcmin^{-2} reported in Paper III.

We conclude that (1) Lyman break objects in the redshift range $3.0 \leq z \leq 3.5$ represent about 1.3% of all objects to $\mathcal{R} = 25.0$, and 2.0% of all objects in the magnitude range $23.5 \leq \mathcal{R} \leq 25.0$; and (2) the density of $z > 3$ galaxies is not significantly higher in fields including bright high-z QSOs.

5. NEAR-IR EMISSION FROM $z > 3$ GALAXIES

In 1995 October we obtained deep K_s band images of a small subset of the $z > 3$ candidates using the Near Infrared Camera (Mathews & Soifer 1994) on the W. M. Keck telescope. A total of five candidates was observed, with typical integration times of 6000 s; four of the candidates are among those confirmed spectroscopically (see Table 1). The measured K magnitudes (typically measuring rest-frame B or V of the galaxies) of the non-AGN candidates (0000−263 C09 appears to be an AGN) range from $K = 21.3$–22.1, with $2.3 \leq \mathcal{R} - K \leq 3.2$.[10] These colors are consistent with models of continuous star formation which could have begun as early as $\gtrsim$1 Gyr prior to the epoch at which we observe them, and are redder than would be expected if we were seeing instantaneous bursts of star formation (Bruzual & Charlot 1993). A consequence of adopting the *maximum* amount of reddening allowed by the UV colors of the galaxies (§ 3) is a reddening in $\mathcal{R} - K$ of $\sim$0.8 mag; this would lower the ages significantly and formally allow single-burst models younger than a few times 10^7 yr. We regard such short lifetimes as unlikely, since they would imply that we are seeing large numbers of galaxies all bursting simultaneously.

6. IMPLICATIONS

The confirmation of a substantial population of luminous star-forming galaxies at $z > 3$ has considerable implications for our understanding of galaxy formation and evolution. One of the advantages of searching for high-z galaxies in the optical is that one observes directly the far-UV continuum produced by early-type stars (our $\mathcal{R}$ bandpass samples the rest-frame continuum at $\lambda_0 \sim 1600$ Å). Consequently, in the absence of dust (see § 3), relatively minor assumptions are necessary to deduce the formation rate of massive stars and the accompanying production of ionizing photons; this is *not* the case for measurements of [O II] line luminosities which are subject to uncertainties as large as a factor of $\sim$5 (see Gallagher, Bushouse, & Hunter 1989). For the purpose of estimating star formation rates (SFRs) from the observed UV luminosities, we have made use of the calculations by Leitherer, Robert, & Heckman (1995) which are based on ultraviolet libraries of massive-star spectra coupled with an evolutionary synthesis code. We have used the "continuous star formation," rather than "single burst," models; we consider the former case more likely, for reasons given in § 5. For a Salpeter initial mass function with an upper mass cutoff of 80 $M_\odot$, a SFR = 1 $M_\odot$ yr^{-1} produces a specific luminosity at 1500 Å (in the rest frame) $L_{1500} = 10^{40.1}$ ergs s^{-1} Å^{-1}. At $z = 3.25$ (in the middle of the redshift range to which we are sensitive to the detection of Lyman break galaxies), an apparent $\mathcal{R} = 24.5$ (on the AB system) corresponds to $L_{1500} = 10^{41.1}$ ergs s^{-1} Å^{-1} ($H_0 = 50$ km s^{-1} Mpc^{-1}) for $q_0 = 0.5$, and $L_{1500} = 10^{41.6}$ ergs s^{-1} Å^{-1} for $q_0 = 0.05$. The population of Lyman break galaxies we detect is in the range $25.5 \gtrsim \mathcal{R} \gtrsim 23.5$; therefore, the implied star formation rates range from 4–25 h_{50}^{-2} $M_\odot$ yr^{-1} ($q_0 = 0.5$) to 12–75 h_{50}^{-2} $M_\odot$ yr^{-1} ($q_0 = 0.05$), with the weighted average being 8.5 h_{50}^{-2} (25 h_{50}^{-2}) $M_\odot$ yr^{-1} for $q_0 = 0.5$ (0.05).

Assuming that we have uniformly probed the redshift range $3.0 \leq z \leq 3.5$ in our surveys (an assumption that is supported by the results of the spectroscopy), the comoving density of the star-forming galaxies is at least 3.6×10^{-4} h_{50}^3 (6.7×10^{-5} h_{50}^3) Mpc^{-3} for $q_0 = 0.5$ (0.05), or about $\frac{1}{2}$ ($\frac{1}{10}$) of the space density of present-day galaxies with $L > L^*$ for $q_0 = 0.5$ (0.05) (Ellis et al. 1996). The total star formation rate per comoving volume produced by the *observed* population at $z > 3$ is then 3.1×10^{-3} h_{50} (1.8×10^{-3} h_{50}) $M_\odot$ yr^{-1} Mpc^{-3} for $q_0 = 0.5$ (0.05). These numbers must be viewed as strict lower limits on the total star formation rate at $z > 3$, the fraction arising in only the most actively star-forming objects; taken at face value, the star formation density that we observe is only $\sim$25% of the total star formation rate seen at the *present* epoch (Gallego et al. 1995). For comparison, the star formation rates (per object) and star formation densities recently reported by Cowie, Hu, & Songaila (1995b) at $z \gtrsim 1$ are approximately the same as we have observed at $z \gtrsim 3$. However, as we detail in Giavalisco, Steidel, & Macchetto (1996b), the morphology of the objects hosting the large star formation rates seems to be entirely different in the two redshift regimes: the great majority of the $z > 3$ objects have very compact morphologies, with half-light radii in *HST* images of $0''.2$–$0''.4$ (1.5–3 h_{50}^{-1} kpc for $q_0 = 0.5$), and in most cases are relatively "regular" in appearance. As pointed out in Paper III, it will be very interesting to observe how rapidly the surface density of Lyman break objects increases at fainter apparent magnitudes.

In summary, we have discovered a population of star-forming galaxies with redshifts $3.0 \leq z \leq 3.5$ using a color-selection technique whose efficiency is very high, allowing the first *systematic* study of the nature of galaxies at such large redshifts. The space density, star formation rates, morphologies and physical sizes (see Giavalisco et al. 1996b), masses, and early epoch of the galaxy population that we have isolated all support the possibility that we are seeing directly, for the first time, the formation of the spheroidal component in the progenitors of present-day luminous galaxies. The fact that we detect such a substantial population using a flat-UV spectrum selection criterion suggests that dust obscuration may not be an important limiting factor in searches for high-redshift galaxies. In any case, our results demonstrate beyond any doubt that massive galaxy formation was well underway by $z = 3.5$.

[10] The optical passbands are on an "AB"-normalized system, whereas the K magnitudes are the standard system. A flat spectrum (f_ν = constant) source has $\mathcal{R} - K = 1.85$.

REFERENCES

Bruzual, G., & Charlot, S. 1993, ApJ, 405, 538
Calzetti, D., Kinney, A. L., & Storchi-Bergmann, T. 1994, ApJ, 429, 582
Charlot, S. 1996, in ASP Conf. Ser., From Stars to Galaxies, ed. C. Leitherer & U. Fritze–von Alvensleben (San Francisco: ASP), in press
Charlot, S., & Fall, S. M. 1993, ApJ, 415, 580
Chen, W. L., & Neufeld, D. A. 1994, ApJ, 432, 567
Cowie, L. L., Gardner, J. P., Hu, E. M., Songaila, A., Hodapp, K.-W., & Wainscoat, R. J. 1994, ApJ, 434, 114
Cowie, L. L., Hu, E. M., & Songaila, A. 1995a, AJ, 110, 1576
———. 1995b, Nature, 377, 603
Djorgovski, S., Pahre, M., Bechtold, J., & Elston, R. 1996, A&AS abstract
Ellis, R. S., Colless, M., Broadhurst, T., Heyl, J., & Glazebrook, K. 1996, MNRAS, in press
Gallagher, J. S., Bushouse, H., & Hunter, D. A. 1989, AJ, 97, 700
Gallego, J., Zamorano, J., Aragon-Salamanca, A., & Rego, M. 1996, ApJ, 455, L1
Giavalisco, M., Koratkar, A., & Calzetti, D. 1996a, ApJ, in press
Giavalisco, M., Steidel, C. C., & Macchetto, F. 1996b, ApJ, submitted
Guhathakurta, P., Tyson, J. A., & Majewski, S. R. 1990, ApJ, 357, L9
Leitherer, C., Robert, C., & Heckman, T. M. 1995, ApJS, 99, 173
Leitherer, C., Vacca, W. D., Conti, P. S., Filippenko, A. V., Robert, C., & Sargent, W. L. W. 1996, ApJ, submitted
Lilly, S. J., Cowie, L. L., & Gardner, J. P. 1991, ApJ, 369, 79
Lowenthal, J. D., Hogan, C. J., Green, R. F., Woodgate, B. E., Caulet, A., Brown, L., & Bechtold, J. 1995, ApJ, 451, 484
Madau, P. 1995, ApJ, 441, 18
Mannucci, F., Beckwith, S. V., & McCaughrean, M. J. 1994, in Infrared Astronomy with Arrays, ed. I. McLean (Dodrecht: Kluwer), 503
Matthews, K., & Soifer, B. T. 1994, in Infrared Astronomy with Arrays, ed. I. McLean (Dordrecht: Kluwer), 239
Oke, J. B., et al. 1995, PASP, 107, 3750
Pahre, M. A., & Djorgovski, S. G. 1995, ApJ, 449, L1
Pei, Y., Fall, S. M., & Bechtold, J. 1991, ApJ, 378, 6
Pettini, M., Hunstead, R. W., King, D. L., & Smith, L. J. 1995, in QSO Absorption Lines, ed. G. Meylan (Berlin: Springer), 55
Pettini, M., & Lipman, K. 1995, A&A, 297, L63
Pettini, M., Smith, L. J., Hunstead, R. W., & King, D. L. 1994, ApJ, 426, 79
Steidel, C. C., Dickinson, M., & Persson, S. E. 1994, ApJ, 437, L75
Steidel, C. C., & Hamilton, D. 1992, AJ, 104, 941 (Paper I)
———. 1993, AJ, 105, 2017 (Paper II)
Steidel, C. C., Pettini, M., & Hamilton, D. 1995, AJ, 110, 2519 (Paper III)
Thompson, D., Djorgovski, S., & Trauger, J. 1995, AJ, 110, 963
Walborn, N. R., Lennon, D. J., Haser, S. M., Kudritzki, R.-P., & Voels, S. A. 1995, PASP, 107, 104

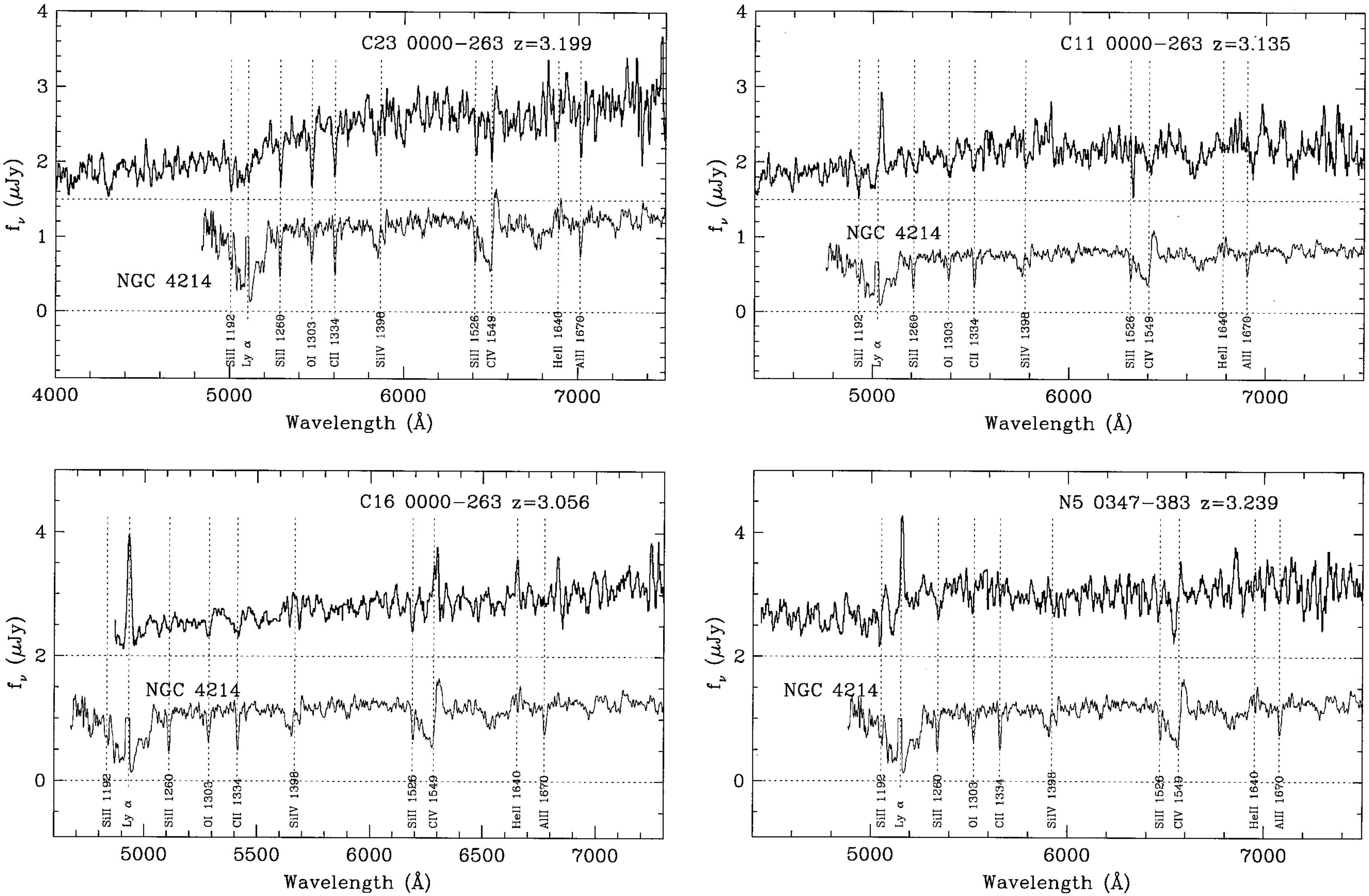

FIG. 1.—Examples of Keck spectra of $z > 3$ galaxies. Below each observed spectrum, we have plotted the spectrum of a star-forming "knot" in NGC 4214, a nearby starburst galaxy (Leitherer et al. 1996), after shifting the spectrum to the measured redshift of the high-z galaxy. Some of the spectral features seen in local star-forming regions (both stellar and interstellar) have been labeled for comparison with the high-redshift objects (see text for discussion). Note that the flux zero point for each high redshift galaxy spectrum is offset relative to the zero point for the scaled spectrum of NGC 4214 (indicated with the second *dotted horizontal line*).